

FATIGUE AT HIGH TEMPERATURE

L. F. Coffin\*

ABSTRACT

*This paper reviews the current state of the art of high temperature fatigue. Attention is given to the relative roles of crack initiation and crack propagation, to damage processes resulting from cyclic strain including that of the substructure, of cyclic strain aging, at grain boundaries, by the environment, from wave shape effects and from plastic instabilities. The phenomenology of high temperature fatigue discussed includes formulation of fatigue equations and material representation, effects of environment, role of frequency, and of wave shape. The state of fatigue life prediction methods is considered with attention given to the most recent approaches to the problem.*

INTRODUCTION

The problem of high temperature fatigue is a complex one. The concern here is with the processes of fatigue crack nucleation and crack growth arising from repeated cycles of load or strain, in specific materials and component geometries, with the added complication of time dependency. In the course of this paper it will be shown that time-dependency at elevated temperature appears in several ways to degrade performance. Further, it is the complexity and specificity of the interaction of these degrading processes together with those of cyclic strain in particular materials that make it difficult to generalize on expected performance.

The importance of the problem in the service performance of a wide range of engineering components is well recognized. The common denominator of cyclic temperature and/or cyclic strain at elevated temperature provides the potential for crack initiation and growth. Many service components are subject to start-stop operations involving elevated temperature, and fatigue in such structures must be carefully considered. Included are aircraft gas turbines, nuclear pressure vessels, heat exchangers and fuel elements, steam turbines and power plant components, etc. Generally such components are designed to perform reliably and safely for predetermined periods of time. An important goal is to provide a satisfactory life prediction criterion for the design life of the component utilizing information obtained in a much shorter time period. Obviously extrapolation is required and an important element in the problem is to select the most appropriate extrapolation or life prediction method.

Any fatigue life prediction method is based either directly or indirectly on the controlling physical processes involved in the fatigue process. We shall try to define some of these processes and how specific materials behave as examples of these processes, utilizing microstructural and

\*Corporate Research and Development, General Electric Co., Schenectady, New York, U.S.A.

phenomenological information as appropriate. The current status of life-prediction methodology will then be considered in the light of this information. Finally some consideration will be given to current trends in the problem, areas of interest for further work and some of the future challenges.

Because of the timeliness and current interest in the topic, there has been much publication activity [1,2] and at least two recent review [3,4] articles on high temperature fatigue. The purpose of the present paper is to update the activity, using as a starting point, more or less, the state of affairs as they prevailed at ICF3 in Munich. Interest in the design of the fast breeder reactor has directed considerable attention to life-prediction methodology and supportive phenomenological activities. As a consequence special attention will be given to this subject.

#### ELEMENTS OF THE PROBLEM

The model shown in Figure 1 has been used earlier to describe the basic elements of the fatigue problem. The crack process is considered to involve three stages: nucleation and early growth, crack propagation through a plastic regime and crack propagation through an elastic regime. These steps in the failure process differ somewhat from those proposed by Forsyth as discussed earlier [4].

The structure shown in Figure 1 contains a notch and a zone of cyclic plastic strain where the nucleation process occurs and where early growth develops. An important topic but one which cannot be considered at length here, [3,5] is the analytical determination of the stress and strain state in the root of the notch. Methods used include (a) use of the pseudo-stress [5,6] (b) the Neuber notch analysis approach, [7,8] (c) finite element analysis [9]. An obviously important aspect of the analytical procedures is to account for the time-dependent deformation i.e., creep. Constitutive equations for such cases are generally formulated in terms of time-independent non-linear deformation, and time-dependent deformation, as well as elastic strains. Accordingly some of the predictive approaches preserve this format in their structure, [3] as will be discussed later.

An important concept in life-prediction methodology is shown in Figure 1(d), where a smooth fatigue specimen is used to simulate the surface strain of the notch. This concept is referred to as "smooth specimen simulation" [7] or the "local strain approach" in translating laboratory data to actual component behavior. The concept is an attractive one in that it permits the massive body of smooth, uniaxially loaded fatigue data to be transferred to the design of the structure, but it is not without its problems. The assumption is made that laboratory specimen failure data are equated to crack initiation in the actual structure. This may be valid when the plastic zone is large relative to the specimen size, or when the strain gradient in the notch is small. Also such factors as biaxiality of stress (plane strain), or surface roughness represent sources of difficulty with the concept. A recent paper by Dowling [10], however, interprets test results from an SAE round-robin test program with service-simulated loading applied to a notched compact-tension specimen, using the local strain approach and finds satisfactory predictive capability. At high temperature the method has been employed by Mowbray and McConneelee [9] and by Coffin [2].

The local strain approach when applied to design assumes that fatigue life is determined by crack initiation, that is, by the situation represented in Figure 1(a). Many engineering structures are designed in

this way. An alternative approach which is finding increasing support with the advent of fracture mechanics concepts in design is to assume the presence of a pre-existing flaw, which negates any contribution from  $N_i$  and assumes that life is a result of  $N_p^D$  or  $N_p^E$  the plastic or elastic crack growth cyclic life. Such procedures are warranted when the probability of defects is high in critically strained regions. Welded structures represent this situation. However, when the volume of similar parts being manufactured is high, when material quality is carefully controlled and when appropriate NDT techniques are employed to reduce the probability to low levels of defect initiated fatigue, then crack initiation concepts are valid.

An intermediate approach is to combine both of the above philosophies. Every effort is taken to ensure that defects are absent from critically-stressed regions and the structure is basically designed by crack initiation. However, to avoid the chance situation of a defect slipping through the inspection process a characteristic defect is assumed and the life so calculated. This quantity serves as the basis for determining the inspection frequency for crack detection of the component.

The point of this discussion relative to the more general thesis of the paper is that we must be concerned with all three of the elements shown in Figure 1 if we are to develop a technical background from which sound predictive procedures can be derived for the reliable performance of real structures subjected to complex loadings and environments.

#### DAMAGE PROCESSES FROM CYCLIC STRAIN

Cyclic plastic strain can be expected to introduce a number of deteriorating processes to the microstructure at elevated temperature depending on the frequency or strain rate. These "damage" processes lead to premature failure by fatigue. A sorting out of available information on this topic is in order.

##### (a) Substructure

Some attention has been given to substructural changes resulting from cyclic strain at elevated temperature. By way of background information, the work of Plumbridge and Ryder [11] and of Feltner and Laird [12] can be cited. A treatment of the substructural changes at elevated temperature was also discussed in reference [4]. The common view is to separate materials into two types, undergoing either wavy or planar slip. Planar slip is favored at low temperature, high frequency, low stress and low stacking fault energy. Increasing temperature promotes wavy slip, leading to a more homogeneous dislocation structure and a decrease in reversible slip [13]. In this transition the favored cyclic strain softening accompanying planar slip can be supplanted by cyclic strain hardening as increasing temperature enhances slip dispersal and the concomitant dislocation substructures developed.

More or less supporting this position is the work of Challenger and Moteef [14] and of Abdel-Raouf, Plumtree and Topper [15]. The latter authors report planar arrays of dislocations for AISI 304 stainless steel at room temperature which change over to elongated cells at 470°C, with a pronounced cellular network at 760°C. Challenger and Moteef found dislocation cells in AISI 304 and 316 stainless steel for temperatures from 430 to 816°C and provided failure occurs in less than  $10^4$  cycles. However, at 430°C and for the 316 stainless steel at low strain, planar arrays were observed.

Both sets of investigators show evidence supporting a correlation between saturation stress (the stress range for a stabilized hysteresis loop) and the inverse of the cell size in the temperature ranges studied. The effect of elevating the temperature was to increase the cell size both for OFHC copper and for austenitic stainless steel, accompanied by a decrease in saturation stress range. Figure 2 shows the behavior for OFHC copper at -75°C, 25°C, 300°C and 600°C [15]. In this figure, the 600°C data are those nearest the origin.

It would appear that studies of the substructure lead to important correlations with the cyclic deformation state, i.e. the relationship between high stacking fault energy, cross slip and the uniqueness of the cyclic stress-strain response independent of strain history, and the distinctions between wavy and planar slip modes and the cyclic stress-strain response. However, correlations between substructure and fracturing processes remain obscure, since, as the temperature is raised the mode of failure shifts from transgranular to intergranular for most materials, particularly at low strain rates. Thus some special features of the grain boundary rather than of the grain must be considered.

#### (b) Cyclic strain aging

Before discussing damage processes leading to intergranular failure, another embrittling effect, that arising from cyclic strain aging should be considered. This phenomenon is most pronounced in carbon steels where the specific hardening and embrittling response is a strong function of temperature, composition, solubility of interstitial carbon and nitrogen and strain rate. As reviewed earlier [4], cyclic strain age strengthening is most noticeable in early cycling and with large strain amplitudes. The mechanism of dynamic strain aging has been recently reviewed by Baird [16] for monotonic deformation and one can presume that the mechanisms in cyclic deformation are similar. Abdel-Raouf, Plumtree and Topper [17] have investigated the cyclic deformation and fatigue behavior of a low-carbon steel. With reference to Figure 3 one notes that a negative strain rate sensitivity regime exists at a cyclic strain range of 2% over temperatures from 100 to 400°C, the effect being strongest at 350°C. The existence of a negative strain rate sensitivity leads to "serrated yielding" discontinuous deformation (Lüders bands) and coarse slip. Concurrently one observes a pronounced decrease in the strain-controlled fatigue resistance in this regime [18]. The two sets of observations would appear to be directly related. The highly localized slip processes lead to early fatigue crack nucleation, and rapid propagation. For example, it has been shown [17] that at 370° mild steel undergoes a decreased fatigue life, brittle striations and non-uniform deformation at low strain rate in contrast to a dimpled fracture surface and homogeneous slip at high strain rates.

When slip is coarse and localized another damaging process, discussed in more detail later, may become important. This is environmental damage. Here crack nucleation from localized oxidation can occur because of the repeated rupture and reforming of protective films due to slip reversal. The effect is most pronounced as the deformation becomes more localized. Examples of this form of damage have been reported earlier [19] and include A286 at temperatures up to 593°C. Evidence has been presented to show that this form of crack nucleation disappears in high vacuum where pronounced life extension is obtained and fracture is largely transgranular [20,21]. A somewhat similar situation is shown in Figure 4 for In 706 [22]. For a plastic strain range of 1.0% the fatigue lives in air and vacuum are

shown as functions of temperature. Note that a dramatic loss in life in the range of 550° -800°C occurs in air, but not in vacuum. The effect is believed to be associated with a localized oxidation process arising from changes in the slip mode. It would be of interest to carry out similar experiments on mild steel in the strain aging regime to see if the slip localization processes and the accompanying decrease in fatigue life associated with strain aging are environmentally influenced.

#### (c) Grain boundaries

Grain boundary migration has been observed for lead [23], iron and for OFHC copper [24] with cyclic strain. In the latter case grain boundaries were observed to orient at directions 40-50° to the stress axis after cycling both at 20°C and 400°C respectively. Snowden, [25] in summarizing the status of this phenomenon in fatigue, points out that migration is essentially complete after about 1% of the expected fatigue life. The result is to develop a "diamond" grain boundary structure acting to increase the grain boundary sliding contribution to the imposed strain.

As an observer of the fatigue process in numerous structural metals at elevated temperature, the author should point out that grain boundary migration is not a very common phenomenon in those metals employed in structural applications. In most alloys, precipitates at grain boundaries act to pin the boundaries to prevent migration and grain boundary sliding. For example AISI 304 stainless steel is not observed to undergo any changes in grain structure at 760°C for strain rates as low as  $2 \times 10^{-4}$  per sec [15]. Thus the damaging effects resulting from grain boundary migration is limited to metals and alloys of high purity, at high homologous temperatures and at low strain rates.

In discussing mechanisms of damage leading to grain boundary fracture in high temperature fatigue, the subject might best be broken down into three categories:

- (i) where grain boundary sliding is significant
- (ii) where intergranular fracture is due to environmental effects
- (iii) where intergranular cracking is a result of neither grain boundary sliding nor of environment.

In case (i) one is concerned with high purity metals and alloys, high homologous temperatures and low strain rates. Damage processes appear to arise from grain boundary migration and triple point cracking as a result of stress concentrations due to sliding for OFHC copper [23]. Cavity nucleation and growth is viewed as an important damage process in this regime, as evidenced by the work of Snowden [26], Westwood and Taplin [24], Williams and Corti [27] and Evans and Skelton [28]. Snowden [25] has reviewed this work and discusses various failure mechanisms proposed for cavity growth. He emphasizes the need for information on the amount of grain boundary sliding and for experimental evidence correlating cavity growth to grain boundary sliding.

#### (d) Environment

A different view of the damage processes in high temperature fatigue has been suggested, based on comparative experiments in air and vacuum [20,21]. The view here is that oxidation is critically important in producing intergranular cracking, since in the absence of an aggressive environment, i.e. a vacuum of  $10^{-8}$  -  $10^{-9}$  torr, fractures tend to be transgranular,

frequency sensitivity is removed and fatigue life is independent of temperature. These effects are shown for A286 at 593°C in Figure 5. Other tests conducted in vacuum on 304 stainless steel at 650°C show no evidence of intergranular fracture at frequencies as low as  $1.6 \times 10^{-4}$  Hz. The view taken here is that the normal processes of crack nucleation and growth which occur at room temperature (or low homologous temperatures) are accelerated in air at elevated temperatures. Freshly exposed surfaces produced by local plastic deformation are rapidly oxidized and serve to further localize the strain, leading to further rupturing and localization accelerating crack nucleation and growth. Grain boundaries are selectively attacked at high temperature because of chemical segregation at grain boundaries and from ready oxidation of grain boundary species, notably carbides. The period of cycle or frequency is important because of the kinetics of the reactions involved. At high frequencies time is insufficient for local chemical reaction and cracking reverts to its normal transgranular mode. At low frequencies or long hold times in tension chemical processes lead to acceleration in the micro- or macrocrack growth rates.

#### (e) Wave form

An important feature of the author's work on environmental effects is the wave form used. In all cases the tests were conducted using a triangular wave form of strain or displacement vs. time in which equal ramp rates in both directions were employed. This so-called "balanced" hysteresis loop would appear to produce failures by fatigue through initiation and growth processes where cracks started at the surface. The environment acted to influence these processes. For example, in air cracks were invariably filled with oxide products, as shown in Figure 6, and were usually intergranular while in vacuum the cracks were transgranular. In no case was any bulk damage observed from the cyclic straining processes.

On the other hand there appears to be evidence to suggest that unbalanced hysteresis loops arising from either unequal ramp rates, from loops involving creep deformation at constant stress in one direction and a rapid reversal (the so-called CP loop) or from tensile strain hold periods, lead to some form of bulk damage process, possibly grain boundary cavity formation, independent of the environment. The evidence for this arises from internal intergranular cracking in tensile strain hold tests in 20Cr-25Ni-Nb stainless steel at 750°C [29] and in a 1CrMoV steel at 565°C [30] where little environmental effect can be expected, intergranular cracking and shortened lives in tests conducted at slow tension and rapid compression going ramp rates in high vacuum [31], and in thermal-mechanical tests conducted in high vacuums where pronounced cavity damage and intergranular cracking was reported [32].

Arguments have been presented [5] to suggest that damage in unbalanced hysteresis loops arises from a deformation ratcheting process of grain boundary sliding associated with slow straining and grain deformation resulting from rapid reverse straining. It would seem more likely that the source of the damage should be more closely associated with creep damage—that is cavity damage which generally occurs on grain boundaries normal to the stress direction and where grain boundary sliding is absent. A view of the damage process that seems consistent with some of the current views regarding cavity damage [33] is one involving nucleation of voids at grain boundaries subjected to normal tensile stresses during some part of the cycle, these voids arising from grain boundary precipitates. It can be argued that such cavities would collapse during the compressive portion of the cycle, such that during balanced hysteresis loops or those involving

compressive hold periods or fast-slow straining (fast tensile strain rate and slow compressive strain rates), those boundaries normal to the loading axis would be free of cavities, while for those wave shapes where tensile stress persists for a longer time than compression (slow-fast, tension strain hold, etc.) cavities would grow with each cycle.

This view is stimulated by recent work of Tipler and Hopkins [34] which showed that significant differences in cavity damage occurred between commercial and high purity Cr-Mo-V steels tested at 550°C. Reductions in trace impurities led to a substantial gain in rupture ductility and life. This improvement was associated with delay in cavitation and reduction in the number of cavities formed by up to two orders of magnitude. McMahon [35] has interpreted these findings from the view that the presence of metalloid impurities enhances the rate of creep cavity nucleation by lowering the cohesion of carbide/ferrite interfaces and increasing the rate of intergranular crack growth by lowering the surface energy of cavities. Hence higher purity reduces cavity nucleation and growth. Our view of the matter is that cavities nucleate and grow on transverse boundaries due to precipitates on the boundary and because of local constraints at the boundary. Quite clearly some work is needed to relate the wave shape effect with specific creep damage processes.

#### (f) Instability

A final form of damage considered here is one which is of a bulk nature rather than arising from substructural or micro-structural considerations. This involves plastic instability arising from second order effects due to cyclic plastic strain. Wigmore and Smith [23] found that vacuum cast copper, rather than failing from triple point cracking as found for OFHC copper, instead underwent a plastic instability and failed by tensile rupture. The process involved is quite similar to that summarized recently by Coffin [36] in considering instability in thermal and mechanical fatigue at elevated temperature. It was shown that the general condition necessary for shape instability is a positional gradient in the cyclic stress-strain field resulting from geometry, temperature or material variation. One of the more interesting effects is the progressive off-center necking that occurs when an hour-glass shaped specimen is subjected to a fast tension going and a slow compression going hysteresis loop wave shape at elevated temperature. When a slow-fast wave shape was introduced, on the other hand, the specimen underwent off-center necking. Sheffler [32] has reported on a similar effect for thermal-mechanical cycling, shown schematically in Figure 7. In these cases, second order effects lead to a slight mean stress component in the off-center position, and this together with a substantially different cyclic stress-strain behavior in the two straining directions leads to a progressive strain ratchet.

#### TESTING METHODS

With the advent of closed loop testing, the experimental opportunities for materials evaluation has been greatly expanded, permitting the experimenter to explore wave shapes of any complexity, fluctuating temperatures and control over a wide range of testing variables including stress, total strain, plastic strain, strain rates, frequencies, etc. Its effect on providing information on material performance has been profound, particularly so at elevated temperature. Some of the possibilities are shown in Figure 8 and include continuous cycling, strain hold tests (either tension, compression or in combination), continuous mean stress cycling, stress

hold, CP or PC types [3], or mixed mechanical and thermal cycling. Test results found for specific materials and temperatures include hysteresis loop stress-strain information, progressive surface and bulk damage information fatigue crack nucleation and propagation, etc., and are useful for specific information for a given material, or in the verification of life prediction criteria. Specimen geometries can be selected according to the objectives of the investigation whether it be directed towards crack initiation or crack propagation.

One of the more important problem areas in high temperature fatigue has been that of time-dependent fatigue, more commonly known as "creep-fatigue". Here the interest is in simulating and predicting performance of materials under conditions typical of actual service. Here the investigator is faced with "time-extrapolation" since both the period of cycling and the total length of time of the service component is often orders of magnitude longer than that which is practical for laboratory testing. Nevertheless it is very important to try to approach service conditions in the laboratory, to the point that experiments in which periods of cycling of an hour or longer will become commonplace and total testing time per specimen will approach months rather than hours.

One of the more interesting wave shape tests useful in evaluating materials in the time-dependent fatigue regime is the so-called slow-fast, equal-equal or fast-slow test, mentioned earlier and shown in Figure 9. The loops shown there reveal how the unequal ramp rates produce non-symmetrical, displaced loops according to the specific stress-strain rate dependence for the material and temperature. The loops shown in Figure 9 are for a normal stress-strain rate dependence. Should the material exhibit inverse strain rate sensitivity as, for example, during strain aging discussed above, loops (b) and (c) would be interchanged.

As discussed above under damage mechanisms, this form of loop provides a very critical evaluation of a given material's sensitivity to wave shape. The strain range partitioning loops known as CP, PC or CC likewise provide this evaluation. However the loops of Figure 9 have several advantages over the SRP loops including ease of control, use of fixed strain rates rather than stress, the attainment of a constant period per cycle, etc.

## PHENOMENOLOGY

### (a) Fatigue equations and their application

It is difficult in the space allotted to this topic to adequately describe the complex phenomenology developed for the cyclic stress-strain and fatigue processes at elevated temperatures. The author has attempted to formalize this complex behavior through the use of the so-called frequency-modified fatigue equations, which represent the material behavior through the use of the plastic (inelastic) strain range and the frequency of the cycle. These equations are:

$$\Delta \epsilon_p = C_2 (N_f v)^{k-1} \quad (1)$$

$$\Delta \epsilon_e = \frac{\Delta \sigma}{E} = A \Delta \epsilon_p^{n'} v^{k_1} \quad (2)$$

$$\Delta \epsilon_e = \frac{\Delta \sigma}{E} = A' N_f^{-\beta'} v^{k_1'} \quad (3)$$

The coefficients for these equations are determined from regression analysis procedures utilizing available test data from smooth, uniaxially loaded specimens tested at specific temperatures, strain ranges and frequencies. Specific features and applicability of these equations are described elsewhere [1,2]. Examples of material behavior, described in more detail in reference [1], can be cited, including the cyclic stress-strain behavior as a function of temperature for AISI 304 stainless steel, Figure 10. Note that the frequency is accounted for by transferring it to the left hand side of equation (2) and plotting this parameter as the ordinate in Figure 10. Of interest is the decrease in stress range and cyclic strain hardening exponent with increasing temperature, and the increasing influence of the frequency of cycling on the resistance to cyclic deformation. Equation (2) can also be expressed in terms of the strain rate for cases of equal and constant ramp rates for each leg of the loop. Here

$$\Delta \epsilon_e = \frac{\Delta \sigma}{E} = B \Delta \epsilon_p^{n'_1} \dot{\epsilon}_p^m \quad (4)$$

where  $B = A/2k_1$ ,  $n'_1 = n' - k_1$  and  $m = k_1$ . Equation (2) or (4) may be useful in analytical procedures for elasto-plastic cyclic stress-strain solutions.

The frequency-modified Coffin-Manson equation, equation (1) is useful in characterizing high temperature low-cycle fatigue behavior. It has been found convenient again to transfer the frequency term to the left side in equation (1) and define this parameter as the frequency-modified plastic strain range. Equation (3), called the frequency-modified Basquin equation, can be similarly treated. Application of equation (1) and (3) are shown in Figure 11 for test data on AISI 304 stainless steel continuously cycled at three strain rates and at three temperatures [37].

Several features arising from the effect of increasing temperature on fatigue phenomenology are observed in this figure. We see the increasingly negative slope and the decreasing life of the plastic strain-cycles to failure representation. Increasing temperature and concomitant softening causes a progressive decrease in the elastic strain (or stress range/elastic modulus). With increasing temperature the transition fatigue life  $N_t$  (the life where the elastic and plastic strain ranges are equal) shifts to lower values of life. The role of the transition fatigue life in distinguishing between low-cycle and high-cycle fatigue is treated elsewhere [2]. Also note that increasing temperature has a small effect on the exponent  $\beta'$  which defines the slope of the elastic strain-cycle life line.

From an engineering design viewpoint the total strain range  $\Delta \epsilon$  is a more commonly used quantity since from it is derived the pseudo-stress  $E \Delta \epsilon$ . This can be found by combining equation (1) and (3). Combining the elastic and plastic lines of Figure 11 for two specific-frequencies, 0.16 and  $0.16 \times 10^{-2}$  Hz (10 and  $10^{-3}$  CPM), and the three temperatures Figure 12 results. Note the increasingly strong frequency effects as the temperature is raised and the large differences in life as the total strain range is decreased. For example, at a strain range of 0.003, the life at 0.16 Hz decreases from  $5 \times 10^5$  cycles to  $7 \times 10^3$  a 70 fold decrease for a change in temperature from 450 to 816°C. At  $0.16 \times 10^{-2}$  Hz on the other hand the lives are  $5 \times 10^5$  cycles and 260, a 1900 fold decrease. At this same strain range, changing the frequency by a factor of a 1000 causes a 27 fold decrease in life. It should be pointed out that these comparisons are based on an extrapolation of the test data to lower frequencies on the assumption

that the frequency exponents of equations (1-3) are independent of frequency.

#### (b) Environment

The effect of high vacuum on high temperature fatigue has been discussed earlier and one example of the effect was shown in Figure 5. A more extensive investigation of the influence of vacuum or inert environments on several materials subjected to a balanced hysteresis loops (equal ramp rates for each leg) was reported earlier [2]. They are summarized in Figure 13. Included here are the low-cycle fatigue test results reported many years ago for room-temperature air [38] (the open points) together with a number of high temperature tests run either in high vacuum or a highly purified argon atmosphere (the solid points). In Figure 13 the test results are normalized to the plastic strain range for failure at one cycle, in order to establish a common base for comparison of the slope by eliminating ductility differences. Lines corresponding to various exponents  $\beta$  in equation (1) are also drawn, showing that the test results fit within a scatter band  $0.45 < \beta < 0.60$ , and the bulk of the data between  $0.50 < \beta < 0.55$ . Note that temperatures as high as  $1150^\circ\text{C}$  are employed in some of the experiments. Frequency of cycling for all these data is 0.033 Hz or greater. All fractures reported in these tests were transgranular. These findings show the significant effect of environment in elevated temperature low cycle fatigue. Note again that the loops employed were balanced and as discussed earlier, additional damage from creep effects can be expected from unbalanced loops (unequal ramp rates for each leg).

#### (c) Frequency dependence and structure

The role of frequency and of environment in high temperature fatigue suggests a model which can serve as a framework for describing specific phenomenology [39].

It has been proposed [40,41] that in an air environment at elevated temperature three frequency regimes exist. At very high frequencies, the time for which the fatigue crack is open is too short for any chemical effect to influence the crack growth processes, such that in this regime frequency of cycling has no effect on crack growth. We exclude here any consideration of strain rate dependency on crack tip strain localization. In this regime, from equation (1),  $k = 1$ . At lower frequencies the environment enters into the crack growth processes and  $k$  is a constant where  $0 < k < 1$ . This is the regime where most of the comparative studies of the fatigue behavior in air and vacuum have been made. Based on smooth specimen tests, for example, it was found that  $k = 0.66$  for A286 in air at  $593^\circ\text{C}$ . In this regime there is a progressive change in the mode of fatigue crack growth from transgranular to intergranular as the frequency is lowered. At still lower frequencies, it has been observed [40] that the fracture mode is entirely intergranular, and that, for a specific plastic strain range, the time to failure remains constant independent of frequency. This regime corresponds to  $k = 0$  as discussed above.

Referring now to Figure 14, these three regimes are shown schematically on a plot of the frequency of cycling  $\nu$  vs.  $N_f$  the cycles to failure. The transition frequencies are identified as  $\nu_e$  and  $\nu_m$ . Further, on Figure 14 is shown an upper bound horizontal line representing the fatigue life for a frequency independent, transgranular failure mode situation. Since Figure 14 is assumed to be generally representative of a wide variety of high temperature alloys, without reference to a specific metal or

temperature, the broad range of applicability of this upper bound line to very low frequencies is uncertain. However in the case of an AISI 304 stainless steel, tests have been made to determine the extent of this constant frequency regime. Here smooth bar specimens were subjected to a cyclic plastic strain of 0.01 and with diametrically opposed small sharp notches to initiate cracks very early in life. It was determined, at  $650^\circ\text{C}$  in high vacuum, that the fatigue life was not significantly altered, whether the frequency of cycling was 1 cpm or 0.01 cpm. Thus there would appear to be no intrinsic material behavior even at frequencies as low as  $1.6 \times 10^{-4}$  Hz that would account for the severe life degradation described above.

On the other hand, A286 apparently shows a change in failure mode from a transgranular to intergranular fracture and a corresponding decrease in life at low frequencies even in high vacuum, as found by Solomon and Coffin [41]. They observed that above a critical frequency, identified on Figure 14 as  $\nu_m$ , the failure mode was increasingly transgranular and the life became independent of frequency while below  $\nu_m$  the fracture was intergranular and the behavior was best described by  $k = 0$ , from equation (1).

Thus in Figure 14 the three regimes identified include at high frequency a time independent regime, an intermediate regime where environment sensitivity is controlling, and a low frequency regime where the deformation mode and environment interact. The critical frequency  $\nu_e$  describes the bound between the higher frequency regimes, while  $\nu_m$  defines the transition where the deformation mode changes independent of the environment. The damaging processes in this low frequency regime are of great technological interest.

When fatigue life in air is reduced with decreasing frequency below  $\nu_e$ , the failure mode becomes increasingly intergranular. As discussed above this has been shown to be due principally to environmental interaction. It is believed that a process analogous to stress corrosion or corrosion fatigue is occurring as a consequence of increasing strain localization at grain boundaries. This suggests that the fatigue life could be improved by a) changing the deformation characteristics of the material to reduce the severity of concentrated strain, b) modifying the grain boundary chemistry to increase intrinsic oxidation resistance, c) aligning the grain boundaries perpendicular to the crack growth direction and d) eliminating the environmental interactions.

Notched bar fatigue tests of A-286 were prepared with three specific aging heat treatments designed to alter the  $\gamma'$  size and the homogeneity of deformation. These heat treatments are identified elsewhere [59].

The results of notched fatigue tests on specimens with  $K_t = 3$  testing at  $\Delta\sigma/2 = 414 \text{ MN/M}^2$  (60,000 psi) at three frequencies are shown in Figure 15. The dashed line for the standard treatment represents a regression analysis of results of tests under a variety of notches and stress levels. A strong frequency dependence of life is apparent below about 5 cpm for all heat treatments. However, the lives are substantially different at a given frequency for the different heat treatments. A double aging treatment (#3) in particular shows much less frequency sensitivity than the single lower temperature treatments. There is no systematic effect of hardness although the general premise regarding the increased resistance to environmentally enhanced embrittlement with increased  $\gamma'$  size appears reasonable.

Since for A286 failure at low frequencies was intergranular, elimination of transverse grain boundaries might be expected to increase the life in the low-cycle regime. Accordingly, two notched specimens with  $K_t = 3.0$  were prepared from remelted stock which had been directionally solidified. Clearly a substantial improvement was obtained as seen in Figure 15. Fractography revealed that the crack propagation was interdendritic while the cracks initiated at a number of sites on the surface at polishing marks inclined at  $15^\circ$  to the plane of loading and were accompanied by localized accumulation of oxidation products as shown by the surface photograph, in Figure 16.

If the transverse grain boundaries are retained but the environment is eliminated in A286, the high vacuum test point shown on Figure 15 at  $\nu = 1.6 \times 10^{-3}$  Hz indicates a further improvement. This confirms that most of the frequency dependence observed in air tests is related to the influence of oxidation processes at the crack tip. The failure of the directionally solidified specimens tested in air to last as long as the vacuum test may be attributed in part to the cast structure in which transverse dendrite boundaries become preferred crack propagation sites.

The three heat treatments were compared over a frequency range of .3 to .03 cpm. From these results and the model of Figure 14, it was decided to explore a broader frequency range. Two tests were performed in air, one at 30 cpm (heat treatment #2), the other at 3.5 cpm (heat treatment #3). Referring to Figure 15 it is seen that, as expected, these higher frequency tests show a greater life. To be consistent with the general view developed above, curves can be constructed for each heat treatment which indicate a common convergence point,  $\nu_e$ , corresponding to  $N_f \sim 4000$  cycles and  $\nu \sim 10^3$  cpm. Above this frequency the material can be expected to be environmentally insensitive and independent of frequency. For frequencies approaching  $\nu_e$  the fracture surface would be expected to be largely transgranular. Examination of the fractograph of the 30 cpm test, supported this view.

#### (d) Wave shape effects

A common form of testing at high temperature involves a tensile strain hold period, shown in Figure 8. Berling and Conway [42] among others have employed this wave form to evaluate AISI 304 stainless steel at  $650^\circ\text{C}$ . Results shown in Figure 17 show a drastic decrease in life with increasing hold period. Accompanying the decreased life is an increasing degree of intergranular fracture.

While tensile strain hold periods are generally found to be more damaging than equal hold periods in tension and compression or of compression hold periods only, this last wave shape has been found to be most damaging, particularly in the case of the cast nickel-base superalloys [43]. Arguments for this anomalous behavior have been presented, under the assumption that this behavior occurs only in cases where the inelastic strains in the hysteresis loop is much smaller than the elastic strains. Further, hysteresis loops so generated are unbalanced, and accordingly a mean stress exists which is tensile for compressive strain hold periods and compressive for tensile strain holds. Now, if elastic crack growth arguments are introduced utilizing crack closure, it is believed that a compressive mean stress is less damaging and tensile mean stress is a more damaging situation, such that tensile holds are less damaging than compressive hold periods. As the inelastic strain increases relative to the elastic strain, crack closure differences diminish, and damage due to crack growth during

tensile relaxation becomes controlling.

More complex wave shapes have been studied by Sheffler [32] on A286 and 304 stainless steel utilizing high vacuum and mixed mechanical and thermal cycles. Referring to the key on Figure 18 the cycle included that which was isothermal (ISOT) and one in which involved an interspersed mechanical strain change and temperature change, either in phase (raising the temperature then increasing the strain), identified as TCIPS. Out-of-phase cycling (raising the temperature then decreasing the strain) is identified as TCOPS. Note that for A286 there is little difference between the fast and slow isothermal tests in vacuum, while an appreciable loss of life is found for the mixed thermal and mechanical cycling, particularly under out-of-phase conditions.

Another series of fatigue tests was performed using slow-fast, fast-slow and equal ramp rates (see Figure 9) on A286 and AISI 304 stainless steel in air and high vacuum [31]. The same overall frequency was employed for each wave form. Referring to Figure 19 of special interest is the fact that the slow-fast tests are more damaging and the fast-slow tests less damaging than the equal ramp rates for the strain ranges used. Also noted but not tabulated, was the loop mean stress, which was negative for the slow-fast cycle and positive for fast-slow, in accord with Figure 9. Of particular interest were the high vacuum results which indicated a relatively small increase in life for the slow-fast tests and greater increases for the equal and fast-slow tests, all for the same period. Similar results are found for the 304 stainless steel. Although further confirmation is needed, they indicate that specific wave shapes can lead to more or to less damage independent of environment influences. Grain boundary damage mechanisms discussed earlier would appear to be responsible for much of the life degradation arising from loop unbalance.

#### PREDICTIVE METHODOLOGY

A wide variety of predictive approaches have been developed over the years, for application to designs for high temperature service. Many of these have been reviewed from time to time [1,44]. Because of the evolving physical understanding and phenomenology, the state of predictive methodology is one of change and improvement. Here we will discuss four of the newer methods currently under active study and evaluation.

##### (a) Strain range partitioning

This approach [45] is built around a series of experiments to establish inelastic strain-cycle life relationships for a given material and temperature. Four sets of cyclic life experiments are required identified as PP, CC, CP and PC tests, where P symbolizes plasticity and implies a rapid, constant ramp rate test, while C symbolizes creep and implies testing at constant load. Thus a PP test is one which is fast, balanced and continuously cycled, while a CC test is conducted under reversed creep conditions at fixed tensile and compressive loads. It, too, is balanced. The CP and PC tests are mixed, consisting of one leg (C) of a hysteresis loop at constant load, the reversed leg (P) at a rapid constant ramp rate. These two loops bring in the element of loop unbalance.

A procedure is involved whereby a given complex hysteresis loop is broken down into components of the four basic loops. Then using an approximate linear damage rule, called the interaction damage rule, a prediction of the life for the complex loop is made from the lives of the component

loops. The method is assumed to have broader applicability than to isothermal conditions, based on tests performed at various temperatures in which the CC, CP and PC baseline failure data show an insensitivity to temperature. The assumption is then made that the baseline data are temperature independent, such that thermo-mechanical loading conditions can be included in the predictive scheme.

There are several questions raised by this predictive approach. One is that the method predicts two bounds—one at high frequency, the other at low frequency. This situation is shown in Figure 20 for a CC and CP loading. The upper bound or high frequency saturation of fatigue life is consistent with the model shown in Figure 14, while the lower bound is not. The question of saturation of fatigue degradation with decreasing frequency is of great practical importance, since many components are cycled as infrequently as once a week or longer.

Another question relates to the basic testing method. Since creep is used as the controlling deformation method, the period of each cycle is controlled by the time to achieve a given strain limit, a time which changes as the test proceeds. Aside from the varying period, a more critical question arises when the creep processes are unimportant relative to environmental damage. Here the cyclic periods become extremely long unless very high stresses are employed. Thus damage due to environment is reflected by creep, rather than factored in through the more normal strain controlled testing procedures. This raises serious problems in interpretation as the temperature is lowered still further, i.e. in the regime where mechanical strain and environment alone interact.

#### (b) Method of Ostergren

Ostergren [47] has recently proposed that hold time and frequency effects at elevated temperature can be accounted for by a damage function based on the net tensile hysteresis energy. This damage measure is approximated by the quantity  $\sigma_t \Delta \epsilon_p$ , where  $\sigma_t$  is the maximum stress in the cycle and  $\Delta \epsilon_p$  is the inelastic strain range. The tensile hysteresis energy is employed to account for the fact that low cycle fatigue is essentially a crack growth process, and that crack growth and damage occurs only during the tensile part of the cycle. The use of the tensile stress quantity in conjunction with the plastic strain range provides a means for accounting for loop unbalance, since, for the same inelastic strain, a positive mean stress gives a greater tensile hysteresis energy than a compressive mean stress.

In order to determine fatigue life, the method requires the substitution of  $\sigma_t \Delta \epsilon_p$  in equation (1). Additionally, two cases are treated, one where time-dependent damage is independent of wave shape, the other where damage is dependent on wave shape. The cast nickel base superalloys are considered to be in the former class since in general  $k = 1$  for this class of materials [48], indicating no frequency effect in equation (1). For most other materials the criterion becomes

$$\sigma_t \Delta \epsilon_p N_F^{\beta} v^{\beta(k-1)} = C \quad (5)$$

where

$$v = 1/(\tau_o + \tau_t - \tau_c) \text{ for } \tau_t > \tau_c \quad (6)$$

and

$$v = 1/\tau_o \text{ for } \tau_t < \tau_c \quad (7)$$

where  $\tau_o$  is the time per cycle of continuous cycling,  $\tau_t$  is the tension hold time and  $\tau_c$  is the compression hold time. Figure 21 shows the correlation of equation (5) with test data on AISI 304 stainless steel.

The method is quite new and untested for wave shapes such as those produced by CP or PC procedures or by fast-slow or slow-fast testing. The identification of the damage category for materials would seem somewhat arbitrary, particularly with respect to the cast nickel-base superalloys since they do show a significant influence of wave shape [43].

#### (c) Frequency separation

Frequency separation is another recently developed approach for predicting high temperature fatigue [31,49]. It is an extension of the frequency-modified fatigue approach described earlier. The frequency-modified fatigue approach described earlier. The frequency-modified fatigue equations have been used as a basis for life prediction [1] by assuming that the period of the cycle but not the wave shape influences fatigue life. Sufficient evidence has been presented here and elsewhere to show that the assumption of wave shape independence on fatigue behavior is unsatisfactory. Accordingly two procedures have been introduced to correct for this inadequacy. Each are built around the concept expressed above that fatigue damage arises from the tension going (i.e. where  $\dot{\epsilon}_p > 0$ ) part of the hysteresis loop, and hence separation of each leg of the hysteresis loop into tension going and compression going was required.

The first of these procedures is very simple, requiring only that the frequency term in equation (1) is replaced by that associated with damage, i.e. the tension-going frequency. Actually, it is more straightforward to deal with time quantities rather than frequencies. Thus in equation (1),  $\tau = 1/v = \tau_t + \tau_c$  where  $\tau_t$  and  $\tau_c$  are the tension and compression going times. Since the coefficients in equations (1-3) have been determined for balanced loop conditions, then  $\tau_t = \tau_c$ . By definition  $\tau_t = 1/v_t$ ,  $\tau_c = 1/v_c$ . Thus for balanced loop conditions  $1/v = 2/v_t$  or, equation (1),  $v = v_t/2$ . For any other loop, the tension going time  $\tau_t$  is found, such that  $v = 1/2 \tau_t$  and this is used in equation (1).

The second procedure is more involved since the first procedure does not adequately predict severely unbalanced loop shapes. Reference is made to the loops and nomenclature shown in Figure 9. It is assumed that the actual stress range for loops of unequal but constant ramp rates can be determined from the mean of the stress range for each leg of the loop. Thus  $\Delta \sigma_{SF} = \Delta \sigma_{FS} = (\Delta \sigma_S + \Delta \sigma_F)/2$ , where the subscript refers to slow and fast. Applying equation (2) of the frequency-modified fatigue equations to obtain the stress range for each frequency, one gets

$$\Delta \sigma_{SF} = \Delta \sigma_{FS} = \frac{\Delta}{2} \left[ \left( \frac{v_c}{2} \right)^{k_1} + \left( \frac{v_t}{2} \right)^{k_1} \right] \Delta \epsilon_p^{n'} \quad (8)$$

Equation (8) has been verified to give reasonable predictions of the stress range for loops of unequal rates [50].

It is next assumed that, if the stress range is known, the life can be determined, using equation (3). Substituting equation (8) into equation (3)



to determine the fatigue life, one finds

$$N_f = \left( \frac{A'}{\Delta\sigma_{SF}} \right)^{1/\beta'} \left( \frac{v_t}{2} \right)^{k_1'/\beta'} \quad (9)$$

Note that the coefficients  $A'$ ,  $k_1'$  and  $\beta'$  are obtained from smooth bar, equal ramp rate tests as indicated earlier.

The applicability of the method to a variety of experiments on wave shape effects at high temperature are reported elsewhere [31]. Shown in Figure 22 is the best fit prediction for some 67 tests on AISI 304 stainless steel at 595°C conducted by the Argonne National Laboratory [51] for the wave shapes and hold times indicated. Further verification and other considerations of the method are discussed in more detail elsewhere [31].

#### (d) Damage rate equation

Another very recent addition to the growing family of high temperature fatigue prediction approaches is that of Majumbar and Maiya [52]. The bases for the approach is crack growth and the separation of the growth processes into two distinct relations, depending on whether the externally applied stress is tension or compression. These relations are:

$$\frac{da}{dt} = \begin{cases} a_T |\dot{\epsilon}_p|^m |\dot{\epsilon}_p|^{-k} & \text{for tensile stress} \\ a_C |\dot{\epsilon}_p|^m |\dot{\epsilon}_p|^{-k} & \text{for compression stress} \end{cases} \quad (10)$$

For continuous cycling, equation (10) is integrated over a given plastic strain range. When  $\dot{\epsilon}_p$  is constant, equation (10) and equation (1) are found to be identical. The method has been used to predict fatigue lives for Type 304 stainless steel under various monotonic and cyclic loading conditions.

#### SUMMARY

Rather than summarizing the subject matter presented here it might, instead, be appropriate to present some generalizations regarding the current state-of-the-art of this field of interest and its future directions. Clearly, the subject is a very complicated one involving the interplay of the several time-dependent processes - environment, creep, and metallurgical stability with cyclic deformation. On the other hand considerable progress has been made, largely from a phenomenological viewpoint, in isolating some of the important elements. In particular, the identification of the importance of the wave shape and the intriguing differences in hold time behavior between tension and compression provide challenges for interpretation. Criteria for life prediction should be built on more physically acceptable models than at present utilizing crack growth concepts for their development. The approach of Majumbar and Maiya is certainly a step in this direction. However, more effort is needed of a micro-mechanical nature to identify and to model the specific physical processes associated with crack growth such that constitutive equations describing crack growth are physically sound and have broad geometric generalities.

Great attention has been given to mechanical testing, generally in the determination of the response of a given material to a given wave shape in air environments. This information is of specific engineering value but it does not help much in the building of a broad picture of the physical events which occur during initiation and growth. Carefully planned programs aimed at sorting out the contributions of competing processes are desirable. Experiments conducted in high vacuum or very pure inert environments are particularly useful in that they eliminate one of the contributing variables. More attention needs to be given to microstructural damage processes and in particular to the role of cavity damage in influencing fatigue behavior for different wave shapes. Specific and carefully controlled environments should be studied for their effect on initiation and growth processes. Relative to this last point, the relative roles of the several time dependent processes involved in initiation vs. growth needs sorting out.

All in all there are many more questions requiring answers than that have been answered in high temperature fatigue. This should make for an exciting future for those dedicated to this interesting subject.

#### REFERENCES

1. COFFIN, L. F., Symp. on Fatigue at Elevated Temperature, ASTM STP 520, 1972, 5-34.
2. COFFIN, L. F., James Clayton Memorial Lecture, Proc. Inst. Mech. Eng., London, 188, 1974, 109.
3. MANSON, S. S. and HALFORD, G. R., An Overview of High Temperature Metal Fatigue, Specialists Meeting on Low Cycle Fatigue AGARD-CP-155, 1974.
4. COFFIN, L. F., Fatigue, Annual Review of Materials Science, 2, 1972, 313-348.
5. COFFIN, L. F., Trans. ASME 78, 1956, 527.
6. MANSON, S. S., Thermal Stress and Low Cycle Fatigue, McGraw-Hill, Inc., New York, 1966, Chapter 4.
7. MORROW, J., WETZEL, R. M. and TOPPER, T. H. in Effects of Environment and Complex Load History on Fatigue Life, ASTM STP 462, American Society for Testing and Materials, 1969, 74.
8. HENRY, M. F., SOLOMON, H. D. and COFFIN, L. F., Intern. Conf. on Creep and Fatigue in Elevated Temperature Applications, paper C182/73 1973.
9. MOWBRAY, D. F. and McCONNELLY, J. E., in Cyclic Stress-Strain Behavior Analysis, Experimentation, and Failure Prediction, ASTM STP 519, American Society for Testing and Materials, 1973.
10. DOWLING, N. E., BROSE, W. R. and WILSON, W. K., Fatigue Design, Analysis Procedures and Test Data, Advances in Engineering Series, Society of Automotive Engineers, to be published.
11. PLUMBRIDGE, W. J. and RYDER, D. A., Metal Mater. Met. Rev. 136, 3:321.
12. FELTNER, C. E. and LAIRD, C., Acta Met. 1967, 15:1621.
13. WELLS, C. H., SULLIVAN, C. P. and GELL, M., Metal Fatigue Damage-Mechanisms, Detection and Repair, ASTM STP 495, 1971, 61.
14. CHALLENGER, K. D. and MOTTEF, J., Fatigue at Elevated Temperature, ASTM STP 520, 1973, 69.
15. ABDEL-RAOUF, H., PLUMTREE, A. and TOPPER, T. H., Metallurgical Transactions, 5, 1974, 267.
16. BAIRD, J. D., The Inhomogeneity of Plastic Deformation, American Society for Metals, Metals Park, Ohio, 1973, 191.

17. ABDEL-RAOUF, H., PLUMTREE, A. and TOPPER, T. H., Cyclic Stress-Strain Behavior-Analysis, Experimentation and Failure Prediction, ASTM STP 519, 1973, 28.
18. COFFIN, L. F., Proc. Int. Conf. on Thermal and High Strain Fatigue, The Metals and Metallurgy Trust, 1967, 171.
19. COFFIN, L. F., Trans. Quarterly American Society for Metals, 56, 1963, p. 359.
20. COFFIN, L. F., Corrosion Fatigue: Chemistry, Mechanics and Micro-structure, NACE-2, Natl. Assn. of Corrosion Engrs., Houston, 1972, 590-600.
21. COFFIN, L. F., Met. Trans., 3, 1972, 1777-1788.
22. WOODFORD, D. A., SOLOMON, H. D. and COFFIN, L. F., Proc. Int. Conf. Materials, II, Boston, 1976, 893.
23. WIGMORE, G. and SMITH, G. C., Metal Science Journal, 5, 1971, 58.
24. WESTWOOD, H. J. and TAPLIN, D. M. R., Metallurgical Transactions, 3, 1972, 1959 and 5, 1974, 1701.
25. VEEVERS, K. and SNOWDEN, K. U., Journal Australian Institute of Metals, 20, 1975, 201.
26. SNOWDEN, K. U., Fracture-Second Tewkesbury Conference, Butterworth and Co., Sydney, 1969.
27. WILLIAMS, H. D. and CORTI, C. W., Metals Science Journal, 2, 1968, 28.
28. EVANS, H. E. and SKELTON, R. P., Metal Science Journal, 3, 1969, 152.
29. TOMKINS, B., ASME Symposium on Micromechanical Modelling of Flow and Fracture; Troy, N.Y. Also TRG Report 2686, Reactor Fuel Element Laboratories, UKAEA, Springfields.
30. ELLISON, E. G. and PATERSON, A. G. F., The Institution of Mechanical Engineers, 190, 1976, 333.
31. COFFIN, L. F., Symposium on Creep-Fatigue Interaction, Winter Annual Meeting American Society of Mechanical Engineers, New York, December 1976.
32. SHEFFLER, K. S., Vacuum Thermal-Mechanical Fatigue Testing of Two Iron Base High Temperature Alloys, NASA-CR-134524, January 1974.
33. PERRY, A. J., Journal of Materials Science, 9, 1974, 1016.
34. TIPLER, H. R. and HOPKINS, B. E., Metals Science, February 1976.
35. McMAHON, C. J., Grain Boundaries in Engineering Materials, Proc. Fourth Bolton Landing Conference, Lake George, New York. Claitors Publishing Division, Baton Rouge, 1974, 525.
36. COFFIN, L. F., Instability Effects in Thermal Fatigue, Thermal Fatigue of Materials and Components, ASTM STP 612, in press.
37. BERLING, J. T. and SLOT, T., Fatigue at High Temperature, STP-465 ASTM, 1968, 3.
38. COFFIN, L. F., Internal Stresses and Fatigue in Metals, Elsevier Publ. Co., Amsterdam, 1959, 363-381.
39. WOODFORD, D. A. and COFFIN, L. F., Grain Boundaries in Engineering Materials, Proc. Fourth Bolton Landing Conference, Lake George, New York. Claitors Publishing Division, Baton Rouge, 1974, 421.
40. SOLOMON, H. D., Met. Trans., 4, 1973, 341-347.
41. SOLOMON, H. D. and COFFIN, L. F., Jr., June 1972 Symp. on Fatigue at Elevated Temperatures, Storrs, Conn., ASTM STP 520, 1972, 112-122.
42. BERLING, J. T. and CONWAY, J. B., Effect of Hold-Time on the Low-Cycle Fatigue Resistance of 304 Stainless Steel at 1200 F, First Intern. Conf. on Pressure Vessel Technology, Delft, Holland, 1969.
43. LORD, D. C. and COFFIN, L. F., Jr., Met. Trans., 4, 1973, 1647-1654.
44. CARDEN, A. E., COFFIN, L. F., MANSON, S. S. and SEVERUD, L. K., Time Dependent Fatigue of Structural Alloys-A General Assessment ORNL-5073, 1975, to be published.

45. MANSON, S. S., June 1972 Symp. on Fatigue at Elevated Temperatures, Storrs, Conn., ASTM STP 520, 1972, 744-782.
46. HIRSCHBERG, M. H. and HALFORD, G. R., NASA TMX-71691, April 1975.
47. OSTERGREN, W., Journal of Testing and Evaluation, ASTM, 4, 1976, 327.
48. COFFIN, L. F., Met. Trans., 5, 1974, 1053-1060.
49. COFFIN, L. F., Proc. International Conference on Materials, II, Boston, 1976, 866.
50. COFFIN, L. F., unpublished research, 1976.
51. WEEKS, R. W., DIERCKS, D. R., CHENG, C. F., ANL Low Cycle Fatigue Studies-Programs Results and Analysis-ANL 8009, November 1973.
52. MAJUMDAR, S. and MAIYA, P. S., A Unified and Mechanistic Approach to Creep-Fatigue Damage, Proc. International Conference on Materials-II, Boston, 1946, 924.

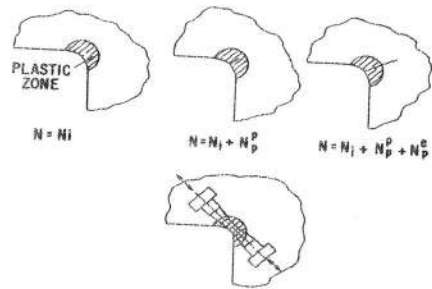


Figure 1 Model for crack initiation and propagation

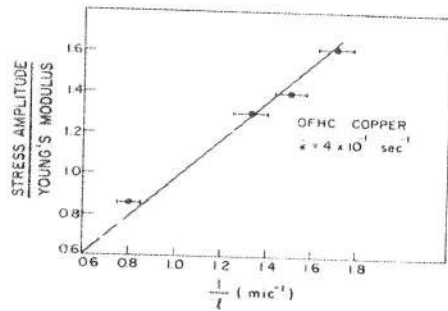


Figure 2 Effect of temperature on cell size for OFHC copper at -75°C, 25°C, 300°C and 600°C. Reference [15]

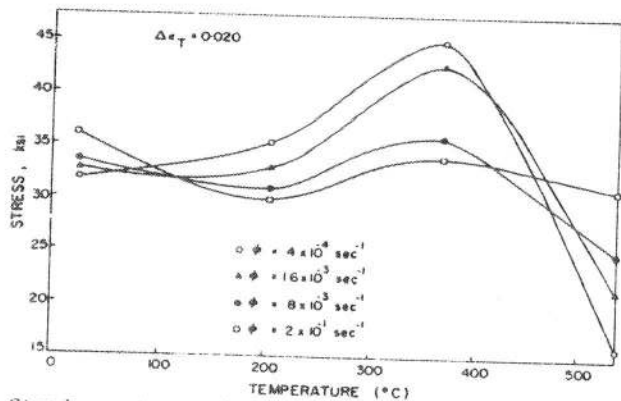


Figure 3 Steady state cyclic stress range vs. temperature for a low carbon steel. Reference [17]

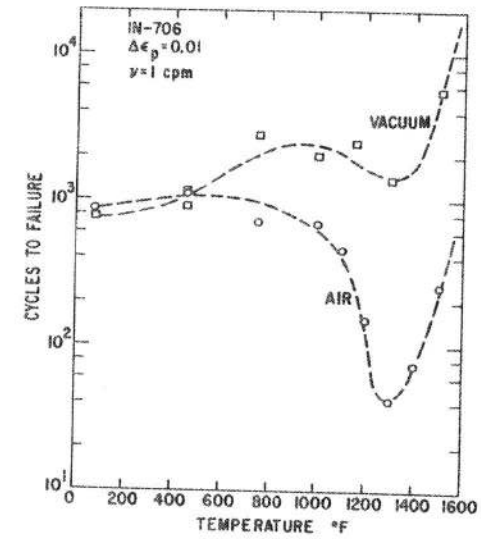


Figure 4 Effect of temperature on cyclic life in air and vacuum for In 706,  $\Delta \epsilon_p = .01$ ,  $\nu = 0.016\text{Hz}$

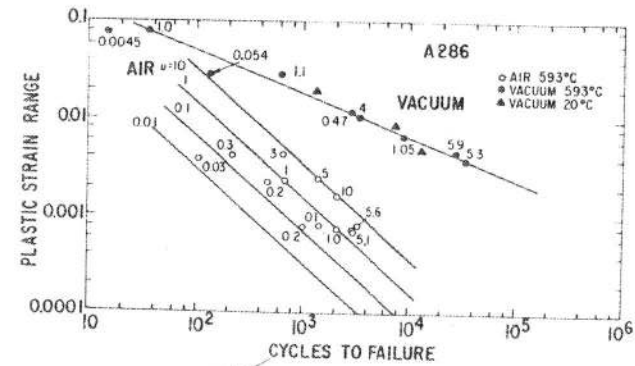


Figure 5 Effect of air and vacuum on low-cycle fatigue behavior of A286 at RT and 593°C at several frequencies

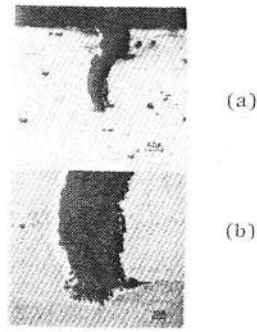


Figure 6 (a) Profile of crack in cast Udimet 500 cycled at 816°C.  
 (b) Detail of tip of crack in (a) showing tendency of localized oxidation to follow grain boundary. Note area of depleted  $\gamma'$  at periphery of oxide.

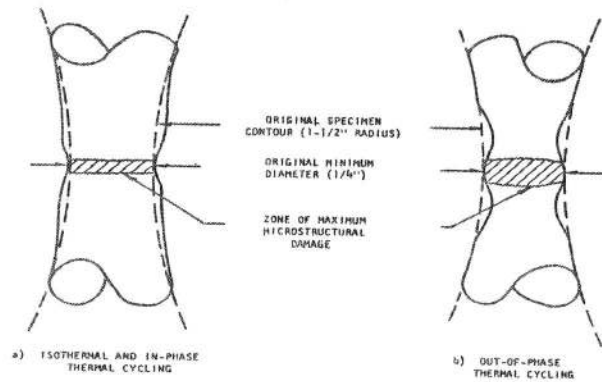


Figure 7 Schematic of shape changes observed with in-phase and out-of-phase cycling of AISI 304 stainless steel. After Sheffler [52].

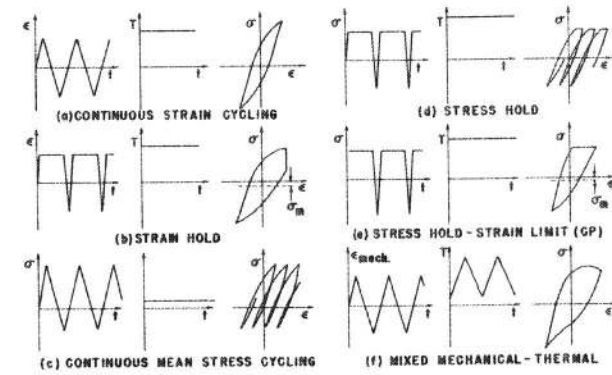


Figure 8 Various wave shapes produced in closed loop testing for life-prediction.

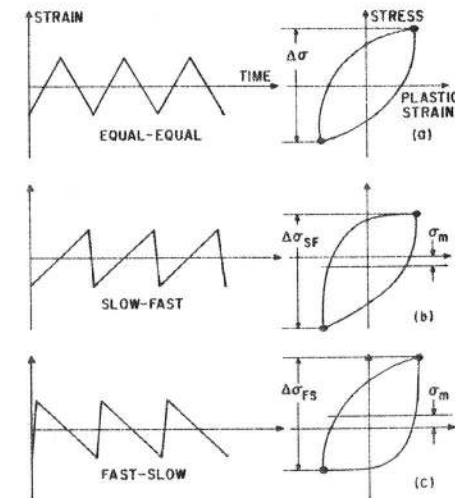


Figure 9 Hysteresis loops resulting from various isothermal wave shapes.

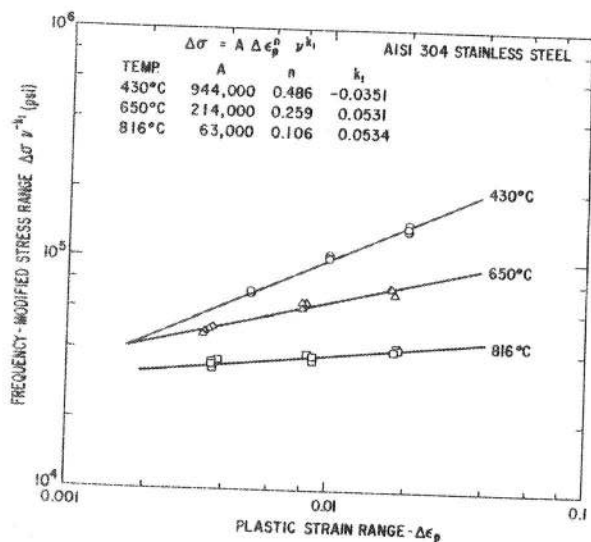


Figure 10 Representation of data of Berling and Slot [37] for 304 stainless steel by equation (2) showing interaction of frequency and stress range in plastic strain range for several temperatures.

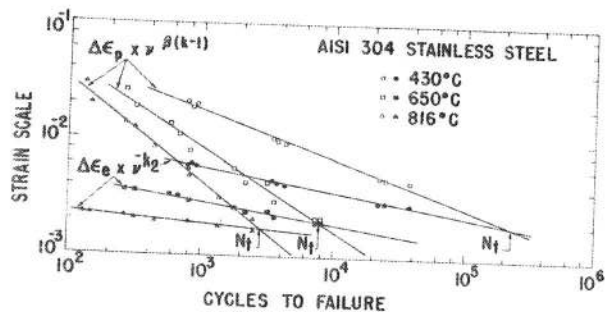


Figure 11 Representation of data of Berling and Slot [37] for 304 stainless steel by equations (1) and (3), showing frequency-modified elastic and plastic strain range at several temperatures in air.  $N_t$  is transition fatigue life.

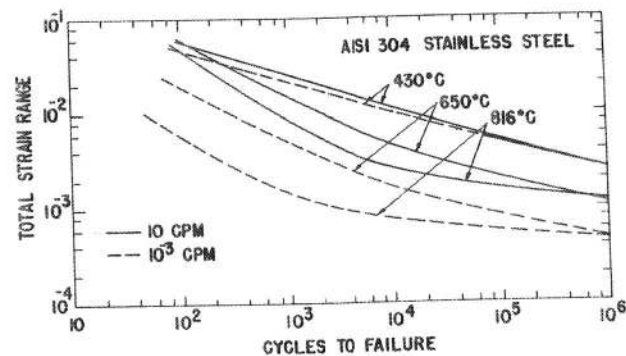


Figure 12 Representation of data of Berling and Slot [37] for 304 stainless steel showing range total strain range vs. cycles to failure for two frequencies at several temperatures in air.

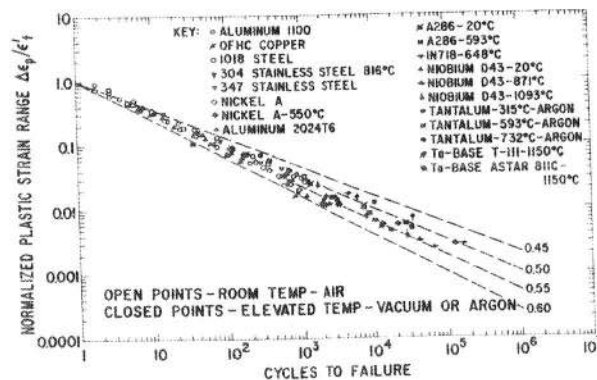


Figure 13 Summary plot of plastic strain range vs. cycles to failure for several metals in room-temperature vacuum or argon. Plastic strain range normalized to fatigue ductility.

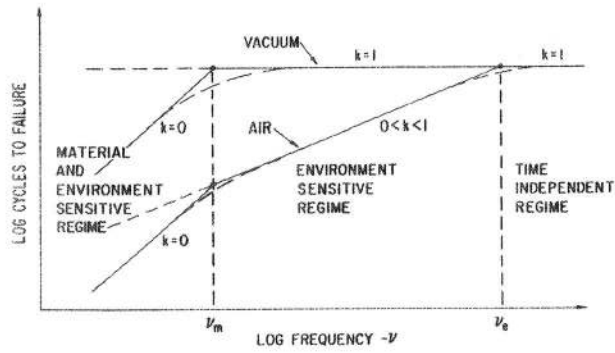


Figure 14 Model of effect of frequency on fatigue life at constant plastic strain range at elevated temperature.

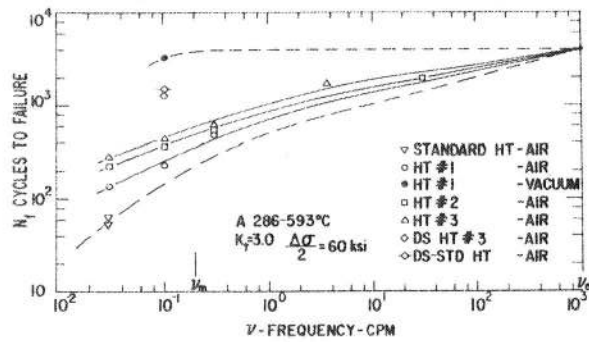


Figure 15 Effect of frequency on life of notched fatigue bars of A286 at 593°C in air and vacuum.

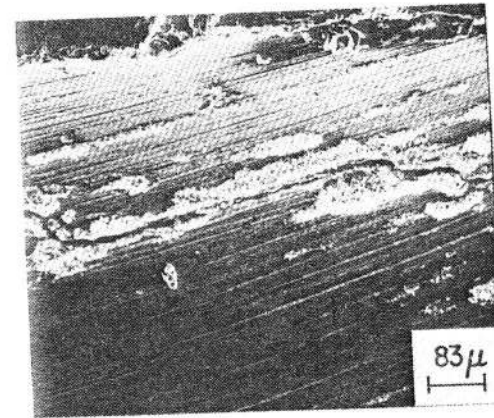


Figure 16 Crack initiation at notch root surface along inclined polishing marks and accompanying localized oxidation-directionally solidified A286 tested in air at 593°C and 0.1 cpm.

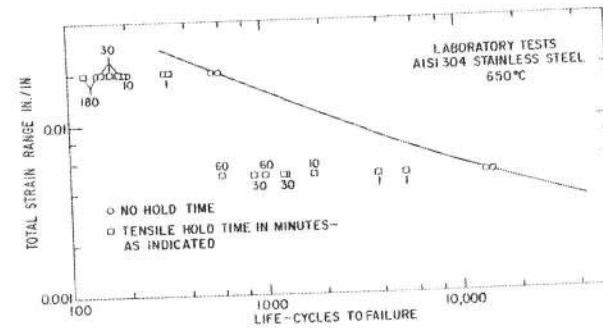


Figure 17 Effect of hold time on life of 304 stainless steel at 650°C. After Berling and Conway [42].

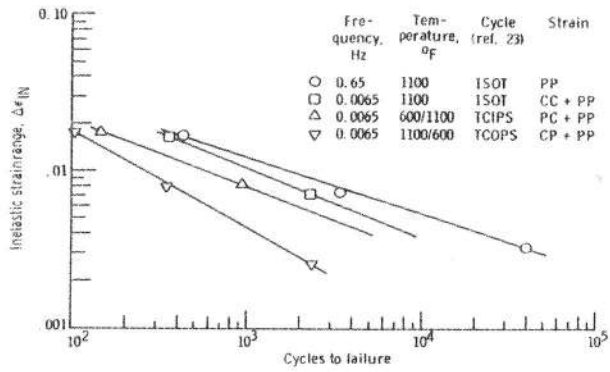


Figure 18 Inelastic strain effects in high vacuum during low cycle fatigue of aged A286, after Sheffler [32].

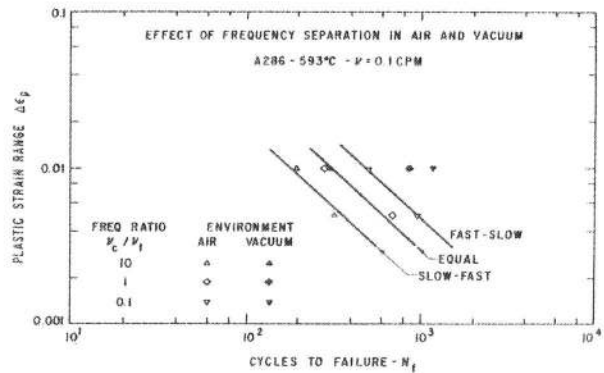


Figure 19 Frequency separation test results in air and vacuum - A286 593°C.

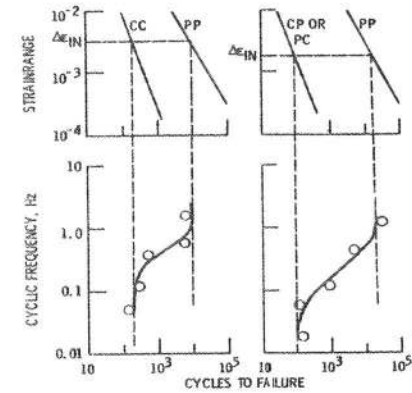


Figure 20 Use of partitioned strain range-life relationships to obtain bounds on life. After reference [45].

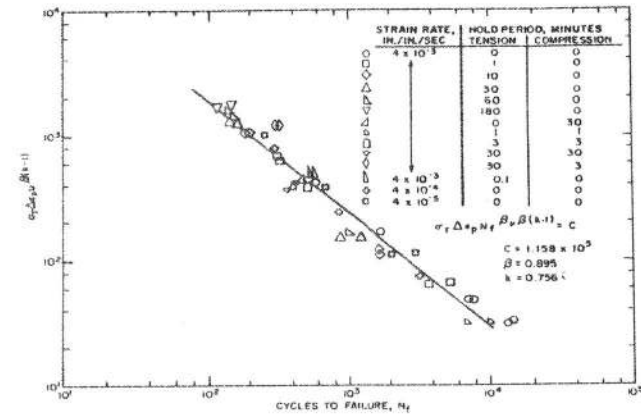


Figure 21 Correlation of AISI 304 stainless steel data with damage function of equation (5), after Ostergren [47].

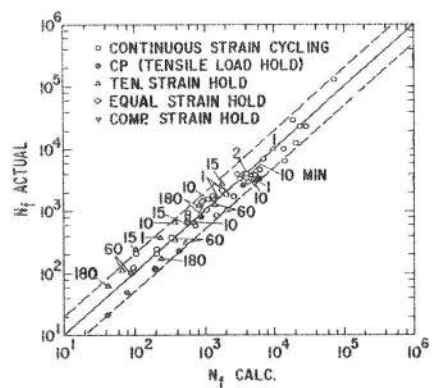


Figure 22 Comparison of actual and predicted lives for AISI 304 stainless steel and 595°C. Reference [31].